



Contents lists available at ScienceDirect

Journal of South American Earth Sciences

journal homepage: [www.elsevier.com/locate/jsames](http://www.elsevier.com/locate/jsames)

## Deep-seated fragmentation, transport of breccia dikes and emplacement: An example from the Borborema province, northeastern Brazil

Valderez P. Ferreira <sup>a,\*</sup>, Alcides N. Sial <sup>a</sup>, Roberto F. Weinberg <sup>b</sup>, Marcio M. Pimentel <sup>c</sup>

<sup>a</sup> NEG-LABISE, Department of Geology, Federal University of Pernambuco, 50740-530 Recife, PE, Brazil

<sup>b</sup> School of Geosciences, Monash University, Melbourne, Australia

<sup>c</sup> Institute of Geosciences, University of Brasília, Brasília, DF, Brazil

### ARTICLE INFO

#### Article history:

Received 31 March 2014

Accepted 18 October 2014

Available online xxx

#### Keywords:

Breccia dike

Xenolith transport rate

Fragmentation processes

Borborema province

### ABSTRACT

Three syenite dike sets, named the Santa Cruz dikes, are coeval with the  $627 \pm 13$  Ma old porphyritic calc-alkalic Princesa Izabel granitoid, northeastern Brazil. Dike set 1 is up to 1.5 m wide, strike 030–040 Az, roughly parallel to the regional foliation. Dike set 2 strikes 120°–130 Az and consists of xenolith-bearing syenites and is roughly parallel to dike set 3, which is up to 1.5 m wide and consists of xenolith-rich syenites forming matrix-supported breccias. Xenoliths in dike sets 2 and 3 are usually up to 3 cm long, angular to sub-rounded, tend to be evenly distributed and occupy ~50% of the volume of dike set 3. They are amphibolite, mica-pyroxenite and diorite from deep source, and gneiss and feldspar xenocrysts from the conduit. The large amount of dense ultramafic/mafic xenoliths in the breccia dikes indicates rapid ascent of the host magma. The calculated natural viscosity, based on whole-rock chemical data, is 680–4600 Pa.s for 2.3 wt% water and temperatures from 1000 to 900 °C, respectively. A minimum ascent rate of ~0.3 m/s is estimated from the settling velocity of a 30 cm-long diorite xenolith, the largest one, and an initial fraction of xenoliths of 5%. Progressive addition of xenoliths to the magma during its ascent increased the viscosity of the liquid–solid mixture during emplacement, and this would imply a Bingham rather than Newtonian behavior. These xenoliths were formed by early fracturing of wall rocks during dike propagation associated with thermal spalling of the wall rocks, by intrusion of magma along dike-parallel fractures during the development of a sequential conjugate pair of shear zones. Xenoliths are abundant not only because these magmas have ascended rapidly and could transport them, but also because the initial low viscosity of the magma promoted intense fracturing of the conduit.

© 2014 Elsevier Ltd. All rights reserved.

### 1. Introduction

The most efficient mechanism by which magma is transported from deep reservoirs to shallow crustal levels seems to be via faults or dikes (e.g. Spera, 1984; Lister and Kerr, 1991; Rubin, 1995; Petford et al., 1993), a process that is supported on thermal and fluid-dynamical grounds (Petford et al., 1994). Most dikes in the upper crust are nearly vertical, although horizontal sheets are also common, and they intrude either pre-existing tensile fractures opened by magma pressure or fill a pre-existing fracture of the host rock. In

this case, the self-propagating magma-filled fractures are normal to the regional direction of least principal stress, the crack propagation rates depending on the activity of volatile components (e.g. Pollard et al., 1975; Spera, 1984; Rubin, 1993, 1995). Brittle-elastic fracturing is a well-known mechanism that allows fast magma migration as dikes through cold crust. Ductile fractures are an alternative for ductile environments, where brittle-elastic diking is inhibited (Weinberg and Regenauer-Lieb, 2010).

Magmatic-hydrothermal breccias are known since long ago as usually associated with hydrothermal ore deposits (e.g. Shelnutz and Noble, 1985; Burnham, 1985; Sillitoe, 1985; Russel et al., 2012). Intrusion breccia dikes result from mechanical fragmentation of wall rocks and subsequent incorporation of fragments, by the intrusive magmas (Sillitoe, 1985). Mechanisms of brecciation and formation of xenoliths include releasing of magmatic

\* Corresponding author. Tel./fax: +55 81 2126 8243.

E-mail addresses: [valderez@ufpe.br](mailto:valderez@ufpe.br) (V.P. Ferreira), [sial@ufpe.br](mailto:sial@ufpe.br) (A.N. Sial), [roberto.weinberg@monash.edu](mailto:roberto.weinberg@monash.edu) (R.F. Weinberg), [marcio@unb.br](mailto:marcio@unb.br) (M.M. Pimentel).

hydrothermal fluid, interaction of ground water with magmas, mechanical disruption of wall rocks, magmatic stoping interactions, dike propagation and emplacement (e.g. Sillitoe, 1985; Rubin, 1993). However, these processes take place mainly in the upper crust. The processes of deep-seated fragmentation and transport of xenoliths are usually associated with kimberlite (e.g. Spera, 1984; Russel et al., 2012) or lamprophyre magmas (e.g. Morin and Corriveau, 1996).

In this study, we focus on the intrusion history of Neoproterozoic breccia dikes with syenitic matrix from northeastern Brazil that form three coeval dike sets carrying different amounts of xenoliths. We discuss the mechanism of rock fragmentation and transport using field descriptions, major element chemistry and theoretical analysis. The dataset provides evidence of a deep-seated mechanism of fragmentation associated with felsic magmas, which is a rare phenomenon, reported for the first time for the Borborema province.

## 2. Regional geology

The Borborema province consists of a complex mosaic of folded crustal segments separated by shear zones. The major features in this province were developed during late Mesoproterozoic to early Neoproterozoic times (Cariris Velhos Event), and late Neoproterozoic times (0.65–0.55 Ga) during the Brasiliano Cycle (Santos, 2000; Brito Neves et al., 2000). A large volume of intermediate to felsic magma was added to the crust during late Neoproterozoic indicating that this orogeny was the major tectonothermal event in the Borborema province (e.g. Ferreira et al., 2004; Van Schmus et al., 2008).

Two EW-trending shear zones, marked by the Patos Shear Zone and Pernambuco Shear Zone, divide the province into three major domains (Fig. 1): (a) North domain, to the north of the Patos shear zone; (b) Central domain also known as Transversal Zone, and (c) the South domain, to the south of the Pernambuco shear zone. These domains are interpreted as representative of a collage of smaller lithotectonic domains (Brito Neves et al., 2000). The Transversal Zone domain is subdivided into sub-domains by

NE–SW dextral transcurrent shear zones that link the Patos and Pernambuco shear zones forming a domino structure. The crustal evolution of this domain has involved the mobilization of significant volume of molten material, preserved as granites and syenites, suggesting high temperatures during the thermal evolution of the region. This thermal activity can be partially related to underplating of mafic magma at the base of the crust, as suggested by coeval granites and syenites with dioritic magma, which occurs as syn-tectonic dikes and co-magmatic intrusions. These rocks present field relationships suggestive of coexistence and local mixing with the host granitoid a feature observed in most batholiths and stocks of this domain (e.g. Sial, 1986; Guimarães and Silva Filho, 1993; Mariano et al., 1996; Neves and Mariano, 1997; Ferreira et al., 1998).

Granitic magmatism in the eastern Borborema province occurred in three main time intervals: (a) 650–610 Ma, (b) 590–570 Ma (largest number and most voluminous plutons), and (c) 550–510 Ma (Ferreira et al., 1998). The oldest plutons consist of magmatic epidote-bearing- high-K calc-alkaline, calc-alkaline and shoshonitic granitoids. The second time interval is marked by abundant intrusions of magmatic epidote-free, high-K calc-alkaline magmas, besides peralkaline, metaluminous high-K syenitic, ultrapotassic, and rare shoshonitic magmas. Peralkaline and rare A-type magmas mark the end of the Brasiliano Cycle in the region at 550–510 Ma (Ferreira et al., 2004). The Santa Cruz dikes are ultrapotassic syenites intrusive into the Princesa Izabel granodiorite, a  $627 \pm 13$  Ma high-K calc-alkaline pluton, part of the oldest group of granitoids, close to the contact with the  $566 \pm 12$  Ma Triunfo ultrapotassic peralkaline syenite (Ferreira et al., 1997), not far from the border between the states of Pernambuco and Paraíba, north of the Santa Cruz village (Fig. 1).

## 3. Chemical, field aspects and relationships of the dike sets

The Santa Cruz intrusions form three dike sets. Dike set 1 (dike 1; Fig. 2a, b) is at least 10 m long and up to 1.5 m wide, striking 030–040 Az, roughly parallel to the regional foliation. They can be disrupted and have either sharp or smooth contours (e.g. Fig. 2b), and is interfingered with the host granodiorite in a feature typical

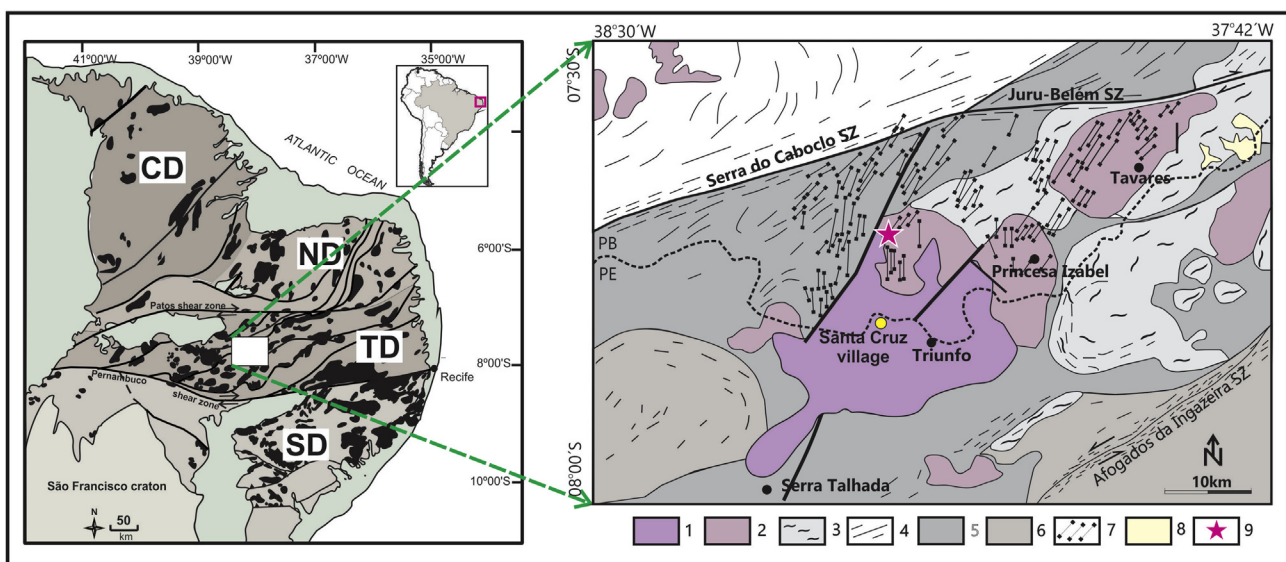


**Fig. 1.** The dike sets: Xenolith-free syenite dike (dike 1; a, b), xenolith-bearing syenite dike (dike 2; c,d) and xenolith-rich (breccia) dike (dike 3; e,f) intrusive into the Princesa Izabel granodiorite. Although sharp, the contacts between dikes and host rock are not rectilinear. Locally, dikes are disrupted and interfingered with the host granodiorite in a typical feature of syn-plutonic dikes (b, e). Dikes 2 and 3 includes small deep-seated mafic as well as the host rock xenoliths. Dikes 1 and 2 show in places thin (1–2 cm) finer-grained margins (Fig. 2d). Arrow in (c) points to a xenolith of the host granodiorite.

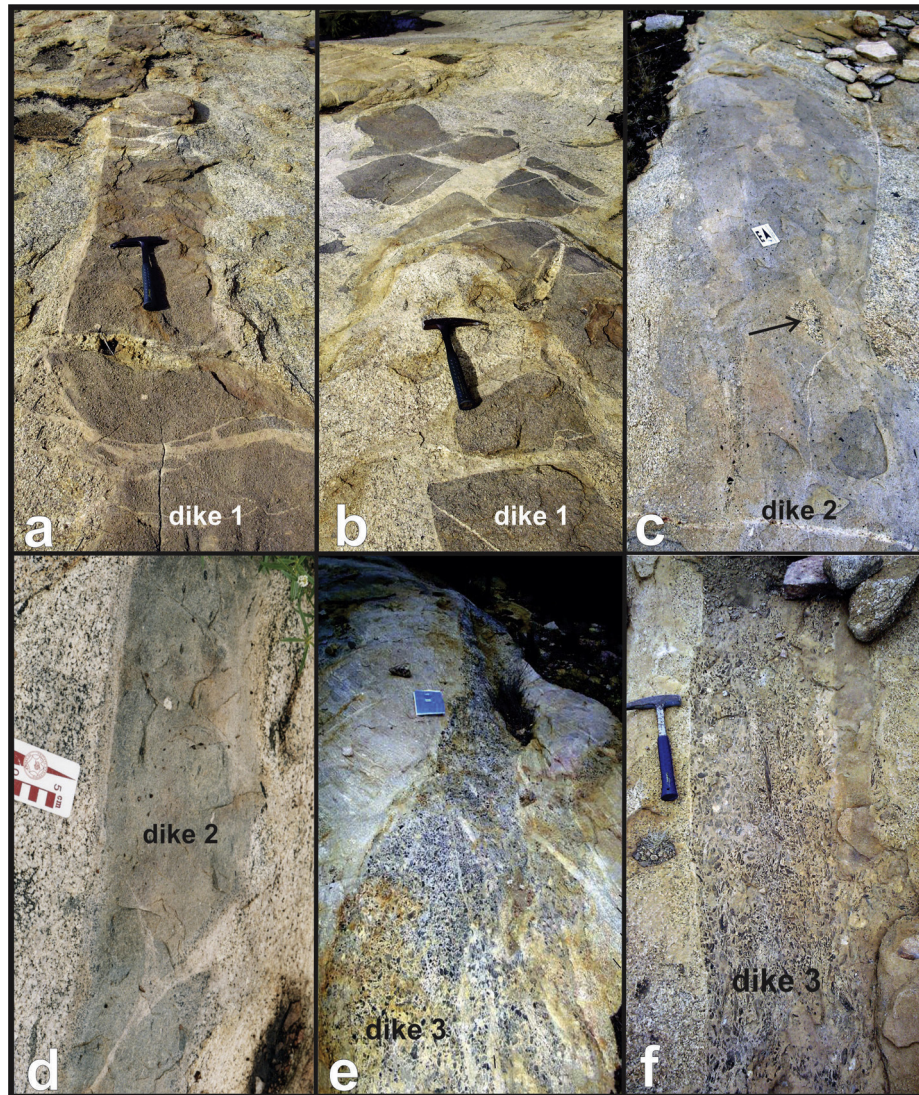


**Fig. 2.** The dike sets: Xenolith-free syenite dike (dike 1; a, b), xenolith-bearing syenite dike (dike 2; c,d) and xenolith-rich (breccia) dike (dike 3) intrusive into the Princesa Isabel granodiorite. Although sharp, the contacts between dikes and host rock are not rectilinear. Locally, dikes are disrupted and interfingering with the host granodiorite in a typical feature of syn-plutonic dikes (b, e). Dikes 2 and 3 includes small deep-seated mafic as well as the host rock xenoliths. Dikes 1 and 2 show in places thin (1–2 cm) finer-grained margins (Fig. 2d).

of syn-plutonic dikes. The second dike set (dike set 2; Fig. 2c, d) strikes 120–130 Az and contains xenoliths of basic igneous, meta-igneous and metasedimentary rocks. Xenoliths are usually small (<3 cm long) and have either random distribution within the dikes or are aligned parallel to their strike. Dike set 2 cuts, sometimes, dike set 1 (e.g. Fig. 3a).

The third dike set (dike set 3) is usually subparallel to dike set 2, cuts dikes 1 and is comprised of matrix-supported breccias in which the matrix has syenitic composition and fragments are xenoliths (Figs. 2e, f, 3b–e). Dikes in this set end in sharp, triangular tips, have strongly irregular, either curved or interfingering margins, indicative of a viscous surrounding. The largest of these intrusions is ~7 m long and up to 1.5 m wide. In these breccia dikes, xenoliths occupy around 50% of the volume, are angular to sub-rounded, commonly up to 3 cm long, and tend to have uniform distribution in the matrix (Fig. 4). Among the xenoliths we have found a slightly foliated diorite of c. 30 cm long (Fig. 4f). Xenoliths at the inner part of the dike are sub-parallel to the dike wall, but closer to the dike wall they are randomly oriented (Fig. 3e), suggesting that

there was flow in the inner portion of the dike while borders tended to cool faster.

The three dike sets contain fragments of the host Princesa Isabel granodiorite (Fig. 2), which in this area is coarse-grained, and locally foliated. The contacts among the intrusions are well-defined although not rectilinear, on the contrary contacts are usually curved and even interfingering (Fig. 3). Dikes 1 and 2 show in places thin (1–2 cm) finer-grained margins (Fig. 2d). The dikes show variable thickness and orientation, and can be oblique to the host rock magmatic foliation, ending as apophysis or abruptly (e.g. Fig. 4a).

The Santa Cruz dikes are made up of medium-to fine-grained orthoclase syenites composed of subhedral perthitic orthoclase and light green diopside (Mg number from 53 to 75) as major phases; titanite, apatite, and rare magnetite are also present. Whole-rock chemical analyses indicate that the syenite is calc-alkaline, metaluminous, potassium-rich with  $K_2O > 6.5$  wt% (average 7.5 wt%),  $K_2O/Na_2O > 2.5$  (average 3.4) and is enriched in large incompatible elements (Ba ~2700–7200 ppm, Rb ~200–260 ppm) (Table 1). The major and trace element concentrations are typical of ultrapotassic

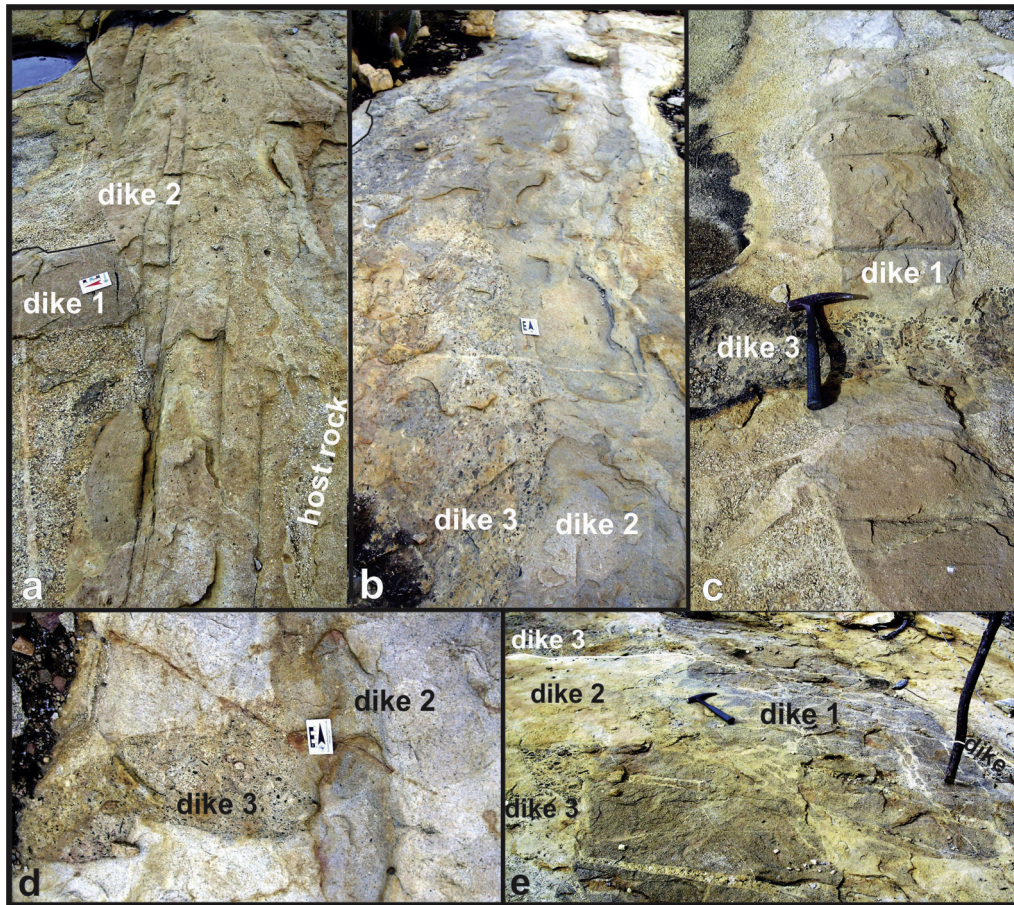


**Fig. 3.** Field relationships between the dikes: (a) dike 2 cuts dike 1; (b) dikes 1, 2, and 3 roughly parallel to each other with no sharp contact; (c) dike 3 cuts dike 1; (d) dike 2 cuts dike 3; dikes 1, 2, and 3 mutually syn-plutonic relative to each other and to the host granodiorite.

rocks in classification schemes such as Foley et al. (1987) and Pecerrillo and Taylor (1976) (Fig. 5). High Nb/Ta ratios (10–104, average 42) and low Rb/Sr ratios (0.22–0.34, average 0.27), besides presence of mantle-derived xenoliths such as pyroxenite, are compatible with the hypothesis that the syenite magma is derived from the mantle.

#### 4. The xenoliths

The xenoliths occupy an average of 50% of the volume of set 3 breccia dikes. Approximately half the xenoliths in dike set 3 are of ultramafic rocks (mainly pyroxenite), 30% are mafic rocks (diorite, amphibolite), and 20% are silica-rich rocks (gneiss, schist), i.e., rocks from both upper mantle and lower/medium crust (Fig. 4). Presence of pyroxenite fragments among the xenoliths but absence of pyroxenite or any other ultramafic rock outcrops anywhere in this region suggests that ultramafic rocks are abundant deep below and that they could have been extracted by the magma.

The xenoliths are angular to subrounded, some of them have oval shape, and they tend to have a regular distribution within the dikes, in random orientation (Fig. 4a–d). Locally, however, xenoliths exhibit a weak preferred orientation in the center of the dikes (Fig. 4e). Schistose xenoliths are usually elongate, and small, with average size of few centimeters. Larger mafic xenoliths can also be observed, the largest one found is a 30 cm long diorite (Fig. 4f). Large (up to 30 cm) xenoliths of the host granodiorite were found in the three dike sets.

Ultramafic xenoliths typically comprise small (up to 3 cm long) subangular mica-pyroxenite composed of augite aggregates and

non-deformed phlogopite, and minor magnetite, apatite, titanite, and interstitial calcite. Some xenoliths are armored by a darker green clinopyroxene layer (mm thick) that has isolated the xenoliths and prevented their further reaction with the liquid. Deformation is not recorded in the minerals of the xenoliths, except for a negligible brittle-ductile deformation.

#### 5. Magma ascent and transport of the xenoliths

The magma flow velocity through a dike depends basically on the width of the dike, viscosity and contrast density between magma and host rock (Rubin, 1995). Ascent velocity can also be affected by the presence of solids in suspension: rigid crystals produce a yield strength that increases the apparent viscosity leading to a non-Newtonian behavior of the magma (Sparks et al., 1977; Caricchi et al., 2007). Most authors relate the occurrence of xenoliths in alkaline magmas to a high ascent velocity, between 10 and  $10^{-3}$  m/s (e.g. Spera, 1984; Maaloe, 1987). The high abundance and lithological diversity of xenoliths in the studied breccia intrusions suggest that the syenite magma had to ascend rapidly through the lithosphere, which allowed for numerous fragments from source and conduits to be extracted and carried up.

In order to estimate the conditions of flow and transport of the syenite magma, which form the groundmass of the breccia dike, and their xenoliths from a deep-magma reservoir to shallower depth, it is necessary to estimate the magma viscosity and density.

The magma viscosity was calculated following the steps of Giordano et al. (2008), using all chemical analyses listed on Table 1. It ranges from 4600 to 74,000 Pa.s at 900 °C and from 680 to

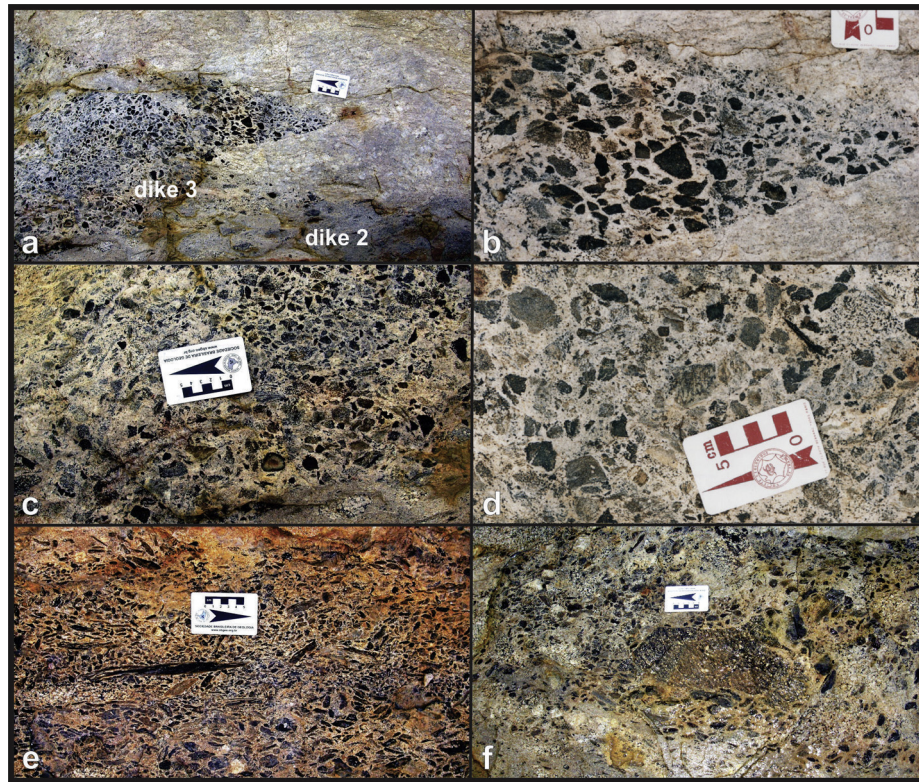


**Fig. 4.** The xenoliths: rock type, size and shape of xenoliths are varied. Xenoliths are usually small, angular to sub-rounded, of unsorted size, and tend to have even distribution within the dike, without preferential orientation (a, b, c, d) and do not touch each other. Elongate xenoliths also are observed, aligned parallel to the dike wall in the inner dike (e). Xenoliths are mainly composed of olivine-free ultramafic and mafic rocks. Figures (a,b) show dike 3 with end tip with sharp contact in one wall and smooth in the other, and corresponds to the crack tip of the dike shown in Fig. 2e. Figure (f) shows a diorite xenolith in the breccia dike that was used for viscosity and velocity calculations in this study.

7700 Pa.s at 1000 °C. Calculated viscosities for the samples listed on Table 1 at different temperatures are shown in the Fig. 6. For the ascent velocity calculation the lower calculated viscosity value was used, i.e. that from sample m2, that has the highest fluorine content and the LOI value was considered as the maximum water content of the magma (Table 1) (see Fig. 7).

The densities of the syenite magma (2.63 g/cm<sup>3</sup> at 900 °C) and of the diorite xenolith rock (2.85 g/cm<sup>3</sup> at 600 °C) were estimated using the method of Bottinga and Weill (1970) and chemical analyses of sample m2 listed in the Table 1.

According to Stoke's Law, the minimum ascent rate of a suspension can be estimated by the sinking velocity of the denser fragment (e.g. Maaloe, 1987; Best, 2003). For a sphere of radius  $r$  moving without interference in a Newtonian magma:

$$v = 2\Delta\rho \cdot g \cdot r^2 / 9\eta \quad (1)$$

where  $g$  = acceleration of gravity (in m/s<sup>2</sup>);  $\Delta\rho$  = density difference between xenolith and magma (in kg/m<sup>3</sup>);  $r$  = radius of the sphere (xenoliths) (in m);  $\eta$  = viscosity of the magma (in Pa.s).

Using the viscosity of sample m2 at 900 °C and density calculated as described above, and the largest diorite xenoliths (30 cm long), the calculated minimum ascent velocity (Equation (1)) is  $v \sim 0.4$  m/s. This is comparable to the ascent rate of garnet/spinel peridotite xenolith-bearing alkali basalt magmas, as estimated by kinetic and fluid dynamics (10<sup>-2</sup> to 10 m/s; Spera, 1984).

A melt containing large amounts of suspended xenoliths may behave rheologically like a Bingham body because xenoliths promote increase of the apparent magma viscosity and yield strength. Therefore, Newtonian viscous behavior, in which the strain rate and shear stress are linearly proportional, is invalidated. The change

from Newtonian to Bingham behavior implies that velocity is diminished due to increased yield strength and viscosity of the magma which provides additional resistance to flow. The sinking velocity of a particle in a liquid containing solid fraction can be calculated using the equation (Shaw, 1969):

$$v = v_0(1 - F)^{4.65} \quad (2)$$

where:  $v_0$  = sinking velocity of a particle in a Newtonian liquid;  $F$  = solid fraction.

For estimating the solid fraction, it was considered that the amount of fragments has progressively increased during magma ascent, fragmentation and capturing of conduit rocks (as suggested by the variety of petrographic types of xenoliths), up to ~50% of the volume of magma at the final emplacement level. Further, assuming that: Most xenoliths are from the upper mantle and/or lower crust; Xenoliths have been fragmented and decreased in size during magma ascent. An initial fraction of xenoliths of ~5% is estimated from the amount of pyroxenite xenoliths, the most ultramafic ones, resulting  $v \sim 0.3$  m/s, at the initial emplacement phase, and  $v \sim 0.02$  m/s at the final phase, with ~50% of solid phase.

The estimated final velocity is much lower than that obtained considering the sinking of an isolated solid in a Newtonian magma.

Similar values are obtained when calculation is done substituting the Newtonian viscosity of Equation (1) by the effective viscosity  $\eta_e$  that is dependent of the solid fraction (Marsh, 1981), considering for the 5% of pyroxenite as solid fraction:

$$\eta_e = \eta(1 - 1.67F)^{-2.5} \approx 5700 \text{ Pa.s} \quad (3)$$

**Table 1**

Representative whole-rock chemical analyses of the Santa Cruz dikes. Samples d1 to d3 are from the xenolith-free dikes; samples m1 and m2 are from the matrix of the breccia dikes. Major elements in wt%; trace elements in ppm. Density and viscosity calculations were based on the analysis of the sample m2. Chemical analyses were performed at the SGS Laboratories, Belo Horizonte, Brazil.

	d1	d2	d3	m1	m2
SiO <sub>2</sub>	59.66	65.71	60.05	65.81	64.36
TiO <sub>2</sub>	0.73	0.31	0.52	0.26	0.38
Al <sub>2</sub> O <sub>3</sub>	13.16	13.53	14.01	13.26	12.27
FeO	1.44	1.05	1.03	1.23	2.01
Fe <sub>2</sub> O <sub>3</sub>	6.29	4.03	5.73	2.96	4.35
MnO	0.13	0.09	0.2	0.05	0.09
MgO	1.35	0.29	1.21	0.99	1.27
CaO	3.85	1.33	3.52	1.7	1.81
Na <sub>2</sub> O	1.82	2.09	2.09	2.39	2.06
K <sub>2</sub> O	7.79	8.31	8.11	6.95	6.27
Cr <sub>2</sub> O <sub>3</sub>	0.03	0.03	0.02	0.04	0.08
P <sub>2</sub> O <sub>5</sub>	0.24	0.13	0.32	0.14	0.17
LOI	1.2	1.16	0.83	0.92	2.28
total	97.69	98.06	97.64	96.7	97.4
F	530	215	410	749	1045
Ba	5708	7142	5225	2660	1833
Sr	918	830	927	582	443
Zr	336	242	268	164	302
V	148	112	119	100	42
Ce	144	144	211	62	128
Hf	7	5	5	3	7
Ho	0.6	0.2	0.9	0.1	0.7
La	107	109	148	67	74
Nb	7	13	5	1.1	8
Nd	59	56	86	23	42
Ni	51	24	31	56	49
Rb	248	282	261	236	201
Sm	10	9	14	3	7
Ta	0.2	0.4	0.1	0.1	0.8
Tb	0.6	0.4	1.1	0.1	0.4
Th	20	8	8	19	29
U	5	2	3	3	4
Y	31	22	43	18	40
Yb	3	2	3	1.3	4

## 6. Discussion: processes of fragmentation and xenolith entrainment

Many theories have been proposed for the origin of breccias associated to intrusion of magmas, but most of them are related to shallow-depth mechanisms. Sillitoe (1985) provided an overview of breccias related to volcanoplutonic arcs discussing possible mechanisms for brecciation. Among them are breccia formation due to releasing of magmatic-hydrothermal fluids, interactions of ground waters with magmas, mechanical disruption of wall rocks, magmatic stoping interactions, fracturing of conduit wall rocks during dike propagation and emplacement, continuous delamination of wall rock by intrusion of magma along dike-parallel fractures, or thermal delamination (e.g. Sillitoe, 1985; Rubin, 1993; Spera, 1984; Morin and Corriveau, 1996; Motoki et al., 2009; Russel et al., 2012).

In evaluating the probable mechanism of rock fragmentation by the Santa Cruz breccia dikes it has to be considered that the majority of fragments is mantle-derived or is from lower crust rocks and that they include many lithological types, which suggest a continuous fragmentation process in a large section of the lithosphere. These features rule out shallow mechanisms such as remobilization of clasts in fault zone (e.g. Bryant, 1968), interaction of rising magma with meteoric water (e.g. Sillitoe, 1985; Shelnut and Noble, 1985) or hydraulic shear fracturing associated with detachment by thermal delamination (Motoki et al., 2009) as major process of fragmentation.

Another hypothesis used to explain brecciation is magmatic stoping. Stopping is a process in which magma provides space for

intrusion by having blocks fall from the roof of the magma chamber and sink to lower parts (Philpotts, 1990; Best, 2003), allowing magma to move vertically or horizontally. Denser blocks of already fractured rocks can sink into the magma and new fractures can be created in the country rocks due to the thermal stress imposed by the intruding magma and by hydraulic fracturing (Marsh, 1982; Best, 2003). In order to be an effective process, the country rocks must be denser than the magma, and be fractured or capable of being fractured, and therefore stoping is limited to the upper part of the crust, a prerequisite not reached by the studied breccia dikes because the xenoliths are mainly made up of mantle-derived and lower crust rocks. Besides, the size of the studied dikes suggests small volume of magma. This implies that the duration of heating of the country rocks is also small and not enough to induce significant thermal stress that would be necessary for allowing detachment of pieces of rocks, their incorporation and transportation by the rising magma. Thus, the hypothesis of magmatic stoping due to thermal stress of magma emplacement (e.g. Furlong and Myers, 1985) fails to explain the formation of the studied breccias.

The Santa Cruz dikes can be roughly parallel to the regional foliation, and locally parallel to the foliation of host rock but they may also change orientation and cut the host granodiorite structure (Fig. 3). Additionally, the high abundance of massive xenoliths indicates that foliation was not a pre-requisite for fragmentation. These features also suggest that the model of dike intrusion filling a pre-existing fracture of the host rock (e.g. Delaney et al., 1986; Bear et al., 1994) does not explain the present case. Conversely, the 90° angle between the orientations of breccia dikes and xenolith-free dikes suggest they have emplaced along a conjugate fracture system (see discussion below).

The crack-tip propagation model seems to apply to the Santa Cruz breccias dikes. In this model, dikes intrude opening a new tensile fracture by magma pressure in the direction perpendicular to the minimum compressive stress,  $\sigma_3$ . Intrusion of magmas through fracture propagation is driven by internal magma pressure. The direction of crack propagation is determined by the orientation of stress at the crack tip (e.g. Pollard, 1987; Rubin, 1995). A dike propagating through a homogenous medium where an ambient stress external to the dike is applied may undergo shear stress on its walls, causing the rotation of  $\sigma_3$  at the crack tip (Pollard, 1987). Three modes of dike propagation, which result in different dike patterns and geometries, have been distinguished depending on the orientation between the shear stress resolved on the dike walls and propagation direction of the dike (Clemente et al., 2007).

An alternative model would be that of continuous delamination or spalling of walls during magma intrusions along fractures parallel to the dike. This mechanism was proposed by Morin and Corriveau (1996) to explain the fragmentation process and xenolith transport of minnete dikes in the Quebec Province, Canada. In their model, xenoliths were formed by early fracturing of wall rock during dike propagation, together with continuous delamination of wall rock by intrusion of magma along dike-parallel fractures.

Most features presented by the Santa Cruz dikes, despite their smaller dike and xenolith sizes compared to those described by Corriveau and Morin, seem to point to a similar model. A mechanism like that would explain the high abundance of xenoliths as due not only to rapid magma ascent (that would allow xenoliths to be carried up) but also to magma intrusion promoting intense fracturing on the host conduit rocks. The xenolith size probably decreased during magma transport and ascent, in particular in the initial diking process. Different abundance of xenoliths could be explained by progressive losing of magmatic ability to fragment and entrain xenoliths during ascent. Similarly to xenolith-rich kimberlite intrusion, whose high xenolith abundance is due rapid ascent associated to exsolution of dissolved volatiles, the breccia

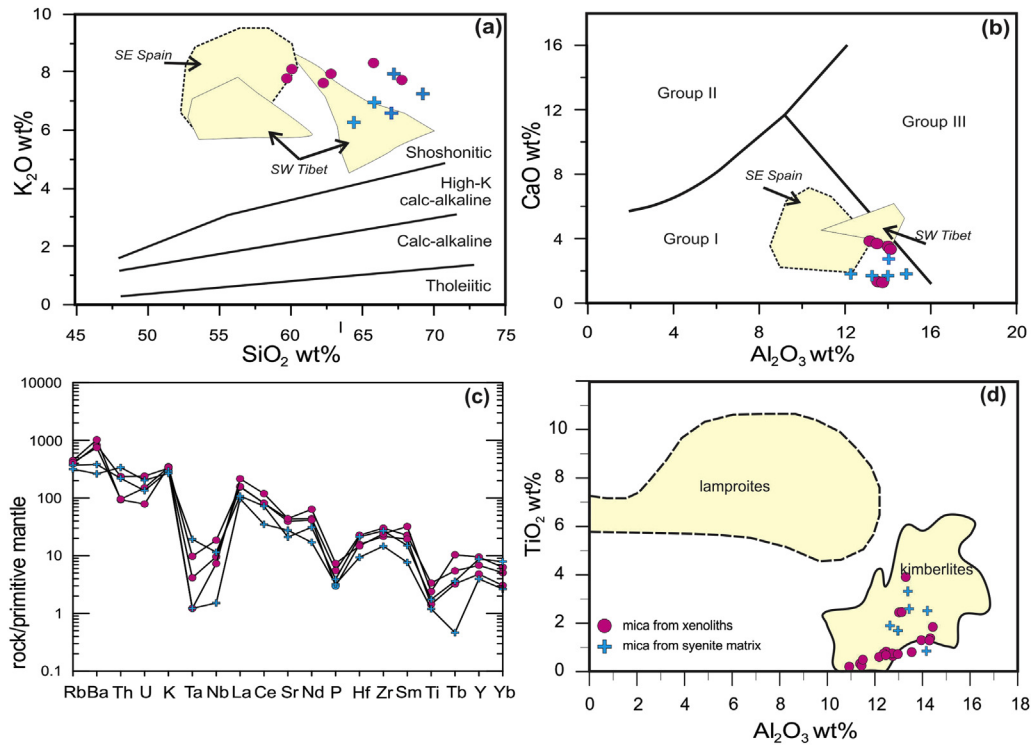


**Fig. 5.** Whole-rock chemical analyses of xenolith-free syenite dikes (circle) and matrix of breccia dikes (cross) on a  $\text{SiO}_2$  versus  $\text{K}_2\text{O}$  diagram (a), with fields of rock series classification of Pecerillo and Taylor (1976); CaO vs  $\text{Al}_2\text{O}_3$  classification diagram (b) for ultrapotassic rocks into groups I (lamproites), II and III after Foley et al. (1987), and primitive mantle-normalized multi-element diagram (c), with normalization factors from Sun and McDonough (1989). Fields for SW Tibet ultrapotassic rocks from Miller et al. (1999) and for lamproites from SW Spain compiled from several authors by Miller et al. (1999) are shown for comparison.  $\text{Al}_2\text{O}_3$  versus  $\text{TiO}_2$  diagram (d) of mica from mica pyroxenite xenolith (circle) and from syenite (cross). Outlined fields for micas from kimberlites and lamproites (Scott-Smith and Skinner, 1984) are shown for comparison.

intrusion was probably initially volatile rich, and the first batch of magma to ascend. Progressive entrainment of fragments during magma ascent would increase the effective magma viscosity, resulting in decreasing magma ascent velocity. This way, the progressive decreasing rate of wall rock fragmentation and their entrainment would give rise to the observed coeval xenolith rich, bearing and free dikes.

In this model, however, breccia dikes would be the first ones to be emplaced, followed by the xenolith-bearing and xenolith-free dikes, although in a short time interval, a sequence not observed in the field. Strike of dikes 1 usually around  $90^\circ$  relative to strike of dikes 2 and 3 is another feature to be considered in the formation and emplacement model. We propose that these features could be explained by magmatic intrusion during the formation of conjugate shears that had a sequential development, that is, each shear zone formed in distinct, although short, time interval (Fig. 3), taking into account the angle between dike strikes, and that one of the dike sets strike ( $030\text{--}040$  Az) is parallel to the regional structure (Fig. 1). The increasing of the effective viscosity of the ascending xenolith-rich dike would lead to a drastic decreasing of the ascending velocity. The bottom lower viscosity xenolith-free magma would look for a new ascending path once the second conjugate shear zone starts forming, this way ascending more rapidly than the xenolith-bearing and xenolith-rich magmas (Fig. 6). Conjugate shear zones usually form at around  $60^\circ$  but can be sequential and initiate at approximate perpendicular orientations (e.g. Mancktelow, 2002; Mitra, 1979; Carreras et al., 2010), and even rotate with increasing deformation. In order to have conjugate sets formed at right angle to  $\sigma_3$ ,  $\sigma_1$  and  $\sigma_3$  should swap around. Alternately, the conjugate sets formed at  $45^\circ$  to  $\sigma_1$  and  $\sigma_3$ . There is field evidence of dike orientation change and rotation, and this makes more likely that the dikes formed at  $45^\circ$  to  $\sigma_1$  and  $\sigma_3$ .

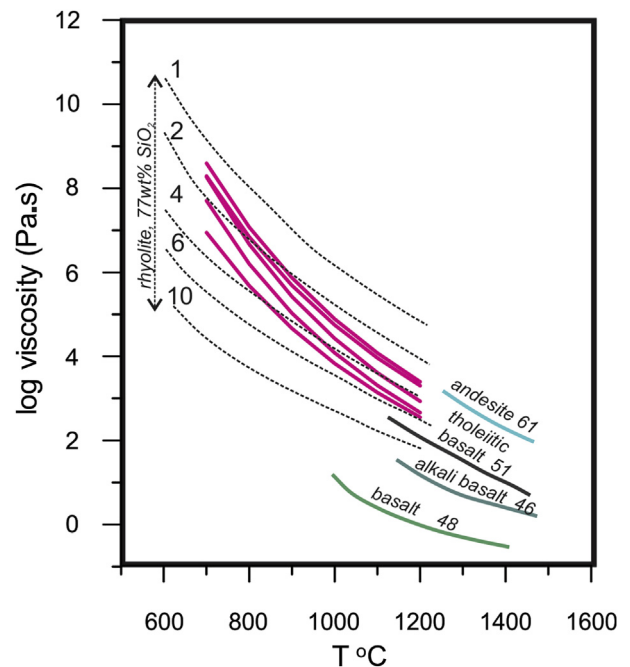


**Fig. 6.** Calculated Newtonian viscosity (pink lines) of xenolith-free and xenolith-rich (breccia) dikes as a function of temperature. Viscosity was calculated after Giordano et al. (2008). Curves for basaltic, andesitic and rhyolite melts at 1 atm as compiled by Best (2003) are shown for comparison. Numbers at the low-T end of the rhyolite curves (dotted lines) are water in weight percentage. (For interpretation of the references to colour in this figure legend, the reader is referred to the web version of this article.)

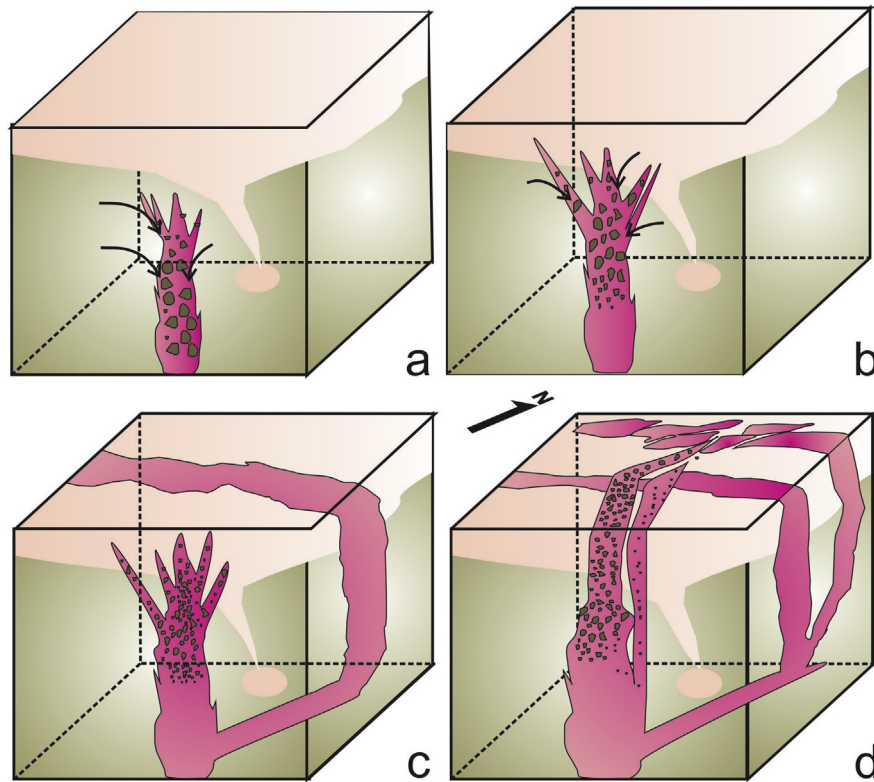


**Fig. 7.** Schematic model of the emplacement of the three dike sets by fracturing of wall rocks during propagation of the dikes in a brittle-ductile sequential development of conjugate shear zones. The first batch of magma ascended very rapid detaching and entraining fragments from the conduit, in continuous delamination of walls during magma ascent. Decreasing fragmentation and entrainment of wall rocks would increase the effective viscosity, decreasing the ascending velocity. The bottom lower viscosity xenolith-free magma takes a new ascending path once the second conjugate shear zone starts forming, ascending more rapidly than the xenolith-bearing and xenolith-rich magmas.

U–Pb zircon LA-ICPMS age of the granite host of the breccia dikes indicates a crystallization age of  $627 \pm 13$  Ma (Ferreira et al., unpublished data); as field relations suggest that they coexisted as magmas for a certain period of time, this implies that this is also the age of emplacement of the syenite breccia dikes. The magma of the breccias dikes is ultrapotassic (Fig. 2a, b) and we speculate about the relationship of this magmatism with that of the ultrapotassic syenitic magmatism expressed by the so-called syenitoid line (SL; Ferreira et al., 1998), a series of plutons emplaced at ca. 570 Ma at the boundary between the Alto Pajeú and Cachoeirinha-Salgueiro terranes (Fig. 1). Olivine-free mica-pyroxenite xenoliths found in the breccia dikes also occur in the 566 Ma Triunfo batholith, the largest ultrapotassic pluton in the SL and in the vicinity of the dikes investigated here (Fig. 1). Micas from xenoliths of the breccia dikes (Fig. 5c) as well as from the Triunfo pluton (see Ferreira and Sial, 1993) have chemistry similar to those of xenoliths from kimberlites, suggesting their mantle origin. It is known that phlogopite melts incongruently under a wide range of conditions producing melts of variable compositions. Experiments conducted by Wyllie and Sekine (1982) show that at depths above 100 km hybridism between cool hydrous siliceous magma rising from subducted oceanic crust, and the hotter overlying mantle peridotite produces olivine-free phlogopite pyroxenite. The Triunfo syenite is considered to be derived from an incompatible element-rich mantle source (Ferreira et al., 1997), and its mica-pyroxenite xenoliths are regarded as derived from the magma source, that probably resulted from hybridization at  $\sim 2.4$  Ga as estimated from Nd model ages (Ferreira et al., 1994). Primitive-mantle normalized multi-variation diagram for the Santa Cruz breccia dikes (Fig. 5d) show enrichment in LIL relative to HFS

elements, and strong Ta, Nb, P and Ti depletions, chemical characteristics ascribed to subduction-related magmatism.

Taken together, we interpret the data as suggestive that the Santa Cruz ultrapotassic syenite magma was formed during an earlier stage of a subduction event at the beginning of the Brasiliano Cycle, in a mantle region close to where hybridism took place producing olivine-free pyroxenite. In a later stage of the Brasiliano cycle, transcurrent movements that followed collision facilitated partial melting of this mica pyroxenite source, which originated the 570 Ma ultrapotassic syenitic magmatism in the region. Although existence of subduction zone at the earliest stages of the Brasiliano Cycle is not a consensus, geodynamic models for the Transversal Zone domain discussed by some authors, such as Brito Neves et al. (2005) and Cabby et al. (2009) invoke a pre-620 Ma subduction setting.

## 7. Concluding remarks

The xenolith-free, xenoliths-bearing and xenoliths-rich (breccia) syenite dikes are coeval with the calc-alkaline granodiorite host rock. Major characteristics of the xenolith-rich (breccias) dikes include: (a) large abundance of xenoliths; (b) small xenolith size (usually  $\sim 5$  cm); (c) dominance of ultramafic/mafic xenolith composition; and (d) maximum dike width of 1.5 m. Progressive addition of xenoliths to the magma during ascent increased the effective viscosity of the liquid–solid mixture during emplacement. Breccia dikes were formed at depth during dike propagation as a result of continuous delamination of the wall rocks by intrusion of magma along dike-parallel fractures and thermal spalling during the development of conjugate shear fractures. Xenoliths are

abundant not only because these magmas have ascended rapidly enough so as to transport source xenoliths, but also because the initial low viscosity of the magma promoted intense physical and thermal disaggregation through fracturing of the conduit.

## Acknowledgments

This study was supported by grants to VPF (CNPq process 476001/2006–4 and FACEPE/PRONEX/CNPq APQ 0479–1.07/06) and to ANS (CNPq 470399/2008, CNPq 472842/2010–2, FACEPE APQ 0727–1.07/08). We are thankful to the two anonymous reviewers for their constructive suggestions. We benefit from discussions with S.P. Neves on an earlier version of the emplacement model. This is the NEG–LABISE contribution n. 263.

## References

- Bear, G., Beyth, M., Rechs, Z., 1994. Dikes emplaced into fractured basement, Timna igneous complex, Israel. *J. Geophys. Res.* 88, 24039–24050.
- Best, M.G., 2003. *Igneous and Metamorphic Petrology*, second ed. Blackwell Pub., p. 729.
- Bottinga, Y., Weill, D.F., 1970. Densities of liquid silicate systems calculated from partial molar volumes of oxide components. *Am. J. Sci.* 269, 169–182.
- Brito Neves, B.B. de, Santos, E.J. dos, Van Schmus, W.R., 2000. Tectonic history of the Borborema province, northeastern Brazil. In: Cordani, U.G., Milani, E.J., Thomaz Filho, A., Campos, D.A. (Eds.), *Tectonic Evolution of South America*, pp. 151–182 (Rio de Janeiro).
- Brito Neves, B.B. de, Van Schmus, W.R., Kozuch, M., Santos, E.J. dos, Petronilho, L., 2005. A zona tectônica Teixeira-Terra Nova – ZTTN – Fundamentos da geologia regional e isotópica. *Geol. USP. Série Científica. São Paulo* 5 (1), 57–80.
- Burnham, W., 1985. Energy release in subvolcanic environments: implications for breccias formation. *Econ. Geol.* 80, 1515–1522.
- Caby, R., Sial, A.N., Ferreira, V.P., 2009. High-pressure thermal aureoles around two Neoproterozoic synorogenic magmatic epidote-bearing granitoids, northeastern Brazil. *J. South Am. Earth Sci.* 27, 184–196.
- Caricchi, L., Burlini, L., Ulmer, P., Gerya, T., Vassalli, M., Papale, P., 2007. Non-Newtonian rheology of crystal-bearing magmas and implications for magma ascent dynamics. *Earth Planet. Sci. Lett.* 264, 402–419.
- Carreras, J., Czeck, D.M., Druguet, E., Hudleston, P.J., 2010. Structure of an anastomosing network of ductile shear zones. *J. Struct. Geol.* 32, 656–666.
- Clemente, C.S., Amorós, E.B., Crespo, M.G., 2007. Dike intrusion under shear stress: effects on magnetic and vesicle fabrics in dikes from rift zones of Tenerife (Canary Islands). *J. Struct. Geol.* 29, 1931–1942.
- Delaney, P.T., Pollard, D.D., Zionym, J.J., McKee, E.H., 1986. Field relations between dikes and joints: emplacement processes and paleostress analysis. *J. Geophys. Res.* 91, 4920–4938.
- Ferreira, V.P., Sial, A.N., 1993. Mica pyroxenite as probable source for ultrapotassic and potassic magmas in northeastern Brazil. *An. Acad. Bras. Ciências* 65, 51–62.
- Ferreira, V.P., Sial, A.N., Whitney, J.A., 1994. Large-scale silicate liquid immiscibility: a possible example from northeastern Brazil. *Lithos* 33, 285–302.
- Ferreira, V.P., Sial, A.N., Long, L., Pin, C., 1997. Isotopic signatures of Neoproterozoic to Cambrian ultrapotassic syenitic magmas, northeastern Brazil: implications for enriched mantle source. *Int. Geol. Rev.* 39, 660–669.
- Ferreira, V.P., Sial, A.N., Jardim de Sá, E.F., 1998. Geochemical and isotopic signatures of Proterozoic granitoids in terranes of the Borborema structural province, northeastern Brazil. *J. South Am. Earth Sci.* 11, 439–455.
- Ferreira, V.P., Sial, A.N., Pimentel, M.M., Moura, C.A.V., 2004. Acidic to intermediate magmatism and crustal evolution in the Transversal Zone, northeastern Brazil. In: Mantesso Neto, V., Bartorelli, A., Carneiro, C. Dal Re, Neves, Brito, de, B.B. (Eds.), *Geologia do Continente Sul-americano: a evolução da obra de Fernando Flávio Marques de Almeida*. Editora São Paulo, pp. 189–201. USP, capítulo XII.
- Foley, S.F., Venturelli, G., Green, D.H., Toscani, L., 1987. The ultrapotassic rocks: characteristics, classification, and constraints for petrogenetic models. *Earth Sci. Rev.* 24, 81–134.
- Furlong, K.P., Myers, J.D., 1985. Thermal-mechanical modeling of the role of thermal stresses and stoping in magma contamination. *J. Volcanol. Geotherm. Res.* 24, 189–191.
- Giordano, D., Russell, J.K., Dingwell, D.B., 2008. Viscosity of magmatic liquids: a model. *Earth Planet. Sci. Lett.* 271, 123–134.
- Guimarães, I.P., Da Silva Filho, A.F., 1993. The mineral chemistry of the Brasileiro age Bom Jardim and Toritama shoshonitic complexes, state of the Pernambuco, northeast Brazil. *An. Acad. Bras. Ciências* 65, 83–106.
- Lister, J.R., Kerr, R.C., 1991. Fluid-mechanical models of crack propagation and their application to magma transport in dikes. *J. Geophys. Res.* 96, 10049–10077.
- Mancktelow, N.S., 2002. Finite-element modeling of shear zone development in viscoelastic materials and its implications for localization of partial melts. *J. Struct. Geol.* 24, 1045–1053.
- Mariano, G., Sial, A.N., Cruz, M.J.M., Conceição, H., 1996. The potassic calc-alkalic Itaporanga batholith, northeastern Brazil: mineral chemistry and oxygen isotope data. *Int. Geol. Rev.* 38, 74–86.
- Marsh, B.D., 1981. On the crystallinity, probability of occurrence and rheology of lava and magma. *Contrib. Mineral. Petrol.* 78, 85–98.
- Marsh, B.D., 1982. On the mechanisms of igneous diapirism, stoping and zone melting. *Am. J. Sci.* 282, 808–855.
- Maaloe, S., 1987. The generation and shape of feeder dikes from mantle sources. *Contrib. Mineral. Petrol.* 96, 47–55.
- Miller, C., Schuster, R., Klötzli, U., Frank, W., Purtscheller, F., 1999. Post-collisional potassic and ultrapotassic magmatism in SW Tibet: geochemical and Sr–Nd–Pb–O isotopic constraints for mantle source characteristics and petrogenesis. *J. Petrol.* 40 (9), 1399–1424.
- Mitra, G., 1979. Ductile deformation zones in Blue Ridge basement rocks and estimation of finite strain. *Geol. Soc. Am. Bul.* 90, 935–951.
- Morin, D., Corriveau, L., 1996. Fragmentation processes and xenoliths transport in a Proterozoic minette dike, Grenville Province, Quebec. *Contrib. Mineral. Petrol.* 125, 319–331.
- Motoki, A., Sichel, S.E., Petralis, G.H., 2009. Genesis of the tabular xenoliths along contact plane of the mafic dikes of Cabo Frio area, State of Rio de Janeiro, Brazil: thermal delamination or hydraulic shear fracturing? *Geociências UNESP* 28, 15–26.
- Neves, S.P., Mariano, G., 1997. High-K calc-alkalic plutons in NE Brazil: origin of the biotite diorite/quartz monzonite to granite association and implications for the evolution of the Borborema province. *Int. Geol. Rev.* 39, 621–638.
- Pecerillo, A., Taylor, R., 1976. Geochemistry of Eocene calc-alkaline volcanic rocks from the Alban Hills (Roman comagmatic region) as inferred from trace element geochemistry. *Contrib. Mineral. Petrol.* 58, 63–81.
- Petford, N., Lister, J.R., Kerr, R.C., 1994. The ascent of felsic magmas in dikes. *Lithos* 32, 161–168.
- Petford, N., Kerr, R.C., Lister, J.R., 1993. Dike transport of granitoid magmas. *Geology* 21, 845–848.
- Philpotts, A.R., 1990. *Principles of Igneous and Metamorphic Petrology*. Prentice Hall, p. 498.
- Pollard, D.D., Muller, O.H., Dockstaeder, D.R., 1975. The form and growth of fingered sheet intrusions. *Geol. Soc. Am. Bull.* 86, 351–363.
- Pollard, D.D., 1987. Elementary Fracture Mechanics Applied to the Structural Interpretation of Dykes. In: Halls, H.C., Fahrig, W.F. (Eds.), *Mafic Dyke Swarms*. *Geol. Assoc. Can.*, vol. 34, pp. 5–24. Spec. Pap.
- Rubin, A., 1993. Tensile fracture of rock at high confining pressure: implications for dike propagation. *J. Geophys. Res.* 98, 15919–15935.
- Rubin, A., 1995. Propagation of magma-filled cracks. *Annu. Rev. Earth Planet. Sci.* 23, 287–336.
- Russell, J.K., Porritt, L.A., Lavallée, Y., Dingwell, D.B., 2012. Kimberlite ascent by assimilation-fuelled buoyancy. *Nature* 481, 352–356.
- Santos, E.J., 2000. Tectonic history of the Borborema Province. In: Cordani, U.G., Milani, E.J., Thomaz Filho, A., Campos, D.A. (Eds.), *Tectonic Evolution of the South-american Platform*, pp. 151–182. Rio de Janeiro, 2000.
- Scott-Smith, B.H.S., Skinner, E.M.W., 1984. In: Kornprobst, J. (Ed.), *Kimberlites 1: Kimberlites and Related Rocks*. Elsevier, pp. 255–283.
- Shaw, H.R., 1969. Rheology of basalt in the melting range. *J. Petrol.* 10, 510–535.
- Shelton, J.P., Noble, D.C., 1985. Premineralization radial dikes of tourmalinized fluidization breccias, Julcani district, Peru. *Econ. Geol.* 80, 1622–1632.
- Sial, A.N., 1986. Granite types of Northeast Brazil, current knowledge. *Rev. Bras. Geociências* 16, 54–72.
- Sillitoe, R.H., 1985. Ore-related breccias in volcanoplutonic arcs. *Econ. Geol.* 80, 1467–1514.
- Sparks, R.S.J., Pinkerton, H., MacDonald, R., 1977. The transport of xenoliths in magmas. *Earth Planet. Sci. Lett.* 35, 234–238.
- Spera, F.K., 1984. Carbon dioxide in petrogenesis III: role of volatiles in the ascent of alkaline magma with special reference to xenoliths-bearing mafic lavas. *Contrib. Mineral. Petrol.* 88, 217–232.
- Sun, S.-s., McDonough, W.F., 1989. Chemical and isotopic systematics of oceanic basalts: implications for mantle compositions and processes. *Geol. Soc. Lond.* 42, 313–345. Special Publications.
- Van Schmus, W.R., Oliveira, E.P., da Silva Filho, A.F., Toteu, S.F., Penaye, J., Guimarães, I.P., 2008. Proterozoic links between the Borborema province, NE Brazil, and the Central African Fold Belt. *Geol. Soc.* 294, 69–99. Special Publication.
- Weinberg, R.F., Regenauer-Lieb, K., 2010. Ductile fractures and magma migration from source. *Geology* 38, 363–366.
- Wyllie, P.J., Sekine, T., 1982. The formation of mantle phlogopite in subduction zone hybridization. *Contrib. Mineral. Petrol.* 79, 375–380.